Department
of
APPLIED MATHEMATICS

Trapping of dilute ion components in wells and double wells in higher equatorial magnetic regions: A kinetic theory including collisions, varying background and additional fields

by

Alf H. Øien

Report no. 157

August 2001

UNIVERSITY OF BERGEN
Bergen, Norway

Department of Mathematics
University of Bergen
5008 Bergen
Norway

ISSN 0084-778X

Trapping of dilute ion components in wells and double wells in higher equatorial magnetic regions: A kinetic theory including collisions, varying background and additional fields

by

Alf H. Øien

Report no. 157

August 2001

Trapping of dilute ion components in wells and double wells in higher equatorial magnetic regions: A kinetic theory including collisions, varying background and additional fields

by

Alf H. Øien

Abstract:

The component of the ambipolar field along the magnetic field B, though weak, may, acting together with the gravitational field, give rise to along-B "ambipolar wells" where light ions (test particles) in the ionosphere in equatorial regions are trapped. We also take into account magnetic field wells, especially in cases when the along- and transverse-B velocities of test particles obey $|v_{\parallel}| \ll |v_{\perp}|$. For heavy ions, or, for light ions high up, when the ambipolar trap ceases to function, the along-B ambipolar- and gravitational field effects may combine with the magnetic field trap to form a double well for the along-B movement of test particles. The magnetic field trap and its contribution to the double well may be nearly stationary for particles obeying $|v_{\parallel}| \ll |v_{\perp}|$ even when collisional effects between the test particles and the background plasma are incorporated. Ions trapped in wells like this, may "feel" a varying background, for instance because of Earth rotation, that may be incorporated as time-variation of parameters in the along-B motion. An along-B kinetic equation for groups of test particles is solved both for the case of simple wells and for double wells, including time-varying collisional coefficients and additional fields, and in some cases analytic solutions are obtained. Peculiar along-B distribution functions may arise due to the time-dependency of coefficients and to various combinations of collision- and field parameter values. In particular "breathing" distributions that alternate between wide and narrow forms in phase-space may arise, and also distributions where strange attractors may play some role.

1 Introduction

In general, ionized particles in magnetic fields respond quite differently to forces and force components along and transverse to the magnetic field. In particular, particles are very sensitive to along-B forcing.

In this paper we model ionized test particle evolution including collisions in some parallel-B wells and double wells set up by gravitational-, electric- and magnetic fields, that may be found in higher, mainly equatorial (magnetic) regions.

One particular well at ionospheric equatorial heights may arise due to the parallel-B component of the vertical force on test particles due to a combination of gravity and ambipolar electric field from the background electrons and ions. We consider the background to constitute a stationary and static "fluid" to lowest order. Another well is the more familiar magnetic field well where in order to approximate it by a harmonic well, we assume test particles are highly anisotropic, i.e. $| v_{\parallel} | << | v_{\perp} |$, for parallel and transverse-B velocities. Also evolution of test particles in wells that are combinations of these wells are considered. Under certain conditions combinations of gravity and electric and magnetic forces may give rise to double wells. In the evolution studies only collisions between test particles and background ions and electrons are taken account of, i.e. test particles-neutral particles collisions are neglected since the modellings are for processes rather high up, say at about 500 km and above,

The evolution is found by solving a kinetic equation for groups of test particles, a dilute component of ions. In the "test particle kinetic equation" the above mentioned collisions will be described by a certain, rather simple, Fokker-Planck term which is in accordance with a Brownian particle picture of movement. The term contains frictional and diffusional effects caused by the background plasma. In some examples also effects of additional fields shall be considered. These fields may arise from the background plasma, but then as a perturbation of an overall static and stationary state. It should be noted that particles in a double well, including frictional effects and an oscillating field, under certain conditions may show chaotic behaviour and have strange attractors. Transverse-B effects in the kinetic equation are averaged out and the study is largely along the magnetic field. However, transverse-B effects have been incorporated using slowly time varying coefficients in the along-B study. This variation may reflect a varying background as test particles in the along-B evolution drift equatorially, say, or rotate with Earth. Test particles are considered to arise from a source that is "lit on" at time $t = 0^{+}$. The along-B kinetic equation including a source term is solved as an initial value problem, and in the cases of harmonic wells and

time varying coefficients, an analytic solution for the test particle distribution function has been found. In some other cases that include cases where particles respond to a double-well, numeric solutions are given.

The paper is outlined as follows: In section 2 wells are modelled in equatorial regions using a dipole magnetic field and an immobile (macroscopic) background (to lowest order) on which test particles (assumed more mobile) evolve. Conditions for trapping and detrapping in collisionless cases are discussed for single test particles. Single particle movements are important when we later solve the collisional kinetic equation (a partial differential equation) where particle movements are characteristics in that equation. In section 3 where the kinetic equation for the test particles is set up the collision term in particular is discussed. In section 4 solutions of the kinetic equation in collisionless cases are found, for the harmonic well case and for the double well case, and figures are given for the evolution of the distribution function when particles arise instantaneously at time $t = 0^+$. In section 5 an explicit analytic solution of the collisional kinetic equation is found when we use a harmonic well and include time-varying coefficients to mimic effects of a changing background. Effects of a time-oscillating force field have also been included in the analytic solution. Solutions are shown graphically for two cases that also illustrate some peculiar effects of time-varying collision coefficients, as "breathing" of distribution functions. In this section we also give examples of distribution function evolutions when a double well, an oscillating field and collisions (partly) are included. Parameter choices used in these illustrations are such that strange attractors seem to play a role. Section 6 is a short summary and conclusion.

2 Examples of trapping of test particles in special well- and double well- potentials

2.1 Ambipolar collisionless trapped test particles in higher equatorial regions

2.1.1 Background plasma and ambipolar electric field

The background plasma that test particles evolve on and respond to, consists of electrons and several components of single ionized ion-species. Effects of neutral particles on test particles, in particular collisional effects, are neglected since neutral particle density is quite low at the heights considered. In ionospheric regions that may be relevant for the modelling background ions may still be Oxygen, while higher up lighter ion species dominate, as Hydrogen, and make up the ion component of the background. For the derivation that follows it is assumed the background plasma is in a stationary and static equilibrium. Then balance of forces prevails: in usual notations, when ion and electron temperatures are equal and uniform (T_0), we assume

$$0 = -\kappa T_0 \frac{\partial n_i}{\partial \mathbf{r}} + n_i e\mathbf{E} - n_i m_i \frac{MG}{r^3}\mathbf{r} \tag{1}$$

for each ion species (subscript "i"), and for electrons (subscript "e"),

$$0 = -\kappa T_0 \frac{\partial n_e}{\partial \mathbf{r}} - n_e e\mathbf{E} \tag{2}$$

since gravity on electrons may be neglected here. Quasineutrality is also assumed:

$$\sum_i n_i = n_e . \tag{3}$$

Then from Eqs.(1)-(3) we have

$$\frac{1}{n_e}\frac{\partial n_e}{\partial \mathbf{r}} = -\frac{\overline{m_+}}{2\kappa T_0}\frac{MG}{r^3}\mathbf{r} \tag{4}$$

where $\overline{m_+}$ is a (general height dependent) weighted ion mass, [1]:

$$\overline{m_+} = \frac{\sum_i m_i n_i}{n_e} . \tag{5}$$

The ambipolar electric force from the same equations then becomes

$$e\mathbf{E} = \frac{\overline{m_+}}{2}\frac{MG}{r^3}\mathbf{r} \tag{6}$$

and is seen to point radially outwards.

2.1.2 Parallel-B ambipolar- and gravity forces on test ions in higher ionospheric regions, and collisionless trapping

On the above plasma background a test ion of mass m and charge q (assumed positive) is subject to a resultant electric and gravitational force given by

$$\mathbf{F} = \left(\frac{\overline{qm_+}}{2e} - m\right)\frac{MG}{r^3}\mathbf{r} . \tag{7}$$

Apart from the dependence on density through $\overline{m_+}$ this force is independent of the background density. The condition for the force to point outwards is

$$m < \frac{\overline{qm_+}}{2e} . \tag{8}$$

For instance, if the background plasma consists only of O^+-ions and electrons, single ionized test ions of atomic number less than 8 will all experience an upward force due to the combined ambipolar electric force and gravity. In this case the magnitude of the force field pointing outwards is approximately 0.4 μV/m. Generally this force has a component along the magnetic field: This is in contrast to electric force fields from other sources, as wind

generated electric fields: Though generally much stronger than the ambipolar field, the field component along B from these sources is zero or practically zero, due to either their origin ("convection"-fields) or the very high conductivity along the magnetic field. The weak ambipolar electric field, important for instance in polar wind studies, [2-4], may therefore also be of relevance in a study of the parallel-B dynamics of test particles in equatorial regions of the ionosphere.

Higher up, where the background is composed mainly of protons and electrons, He-test ions, say, will experience a downward pointing force since then $m > \overline{qm_+}/2e$. (This is further studied later).

The dipole magnetic field of Earth can be given as in [5],

$$\mathbf{B}(r,\lambda) = \frac{\mu_0}{4\pi}\frac{M_E}{r^3}(-2\sin\lambda\mathbf{e}_r + \cos\lambda\mathbf{e}_\lambda) \tag{9}$$

and the field lines by

$$r = r_0\cos^2\lambda \tag{10}$$

using radius- and magnetic latitude-coordinates (r,λ). M_E is the Earth dipole moment, and r_0 the crossing of field lines at the magnetic equator. From Eq.(9) the magnitude of B follows,

$$B = \frac{\mu_0}{4\pi}\frac{M_E}{r^3}(1+3\sin^2\lambda)^{1/2}. \tag{11}$$

One then readily calculates the component of the force Eq.(7) on a test ion along the magnetic field line that crosses the magnetic equator at radius $r_0 = LR_E$, where L and R_E are respectively the (magnetic) L-shell value and Earth radius,

$$F_\parallel^E = -\frac{2\sin\lambda}{\sqrt{1+3\sin^2\lambda}}\left(\frac{\overline{qm_+}}{2e} - m\right)\frac{g}{L^2\cos^4\lambda}. \tag{12}$$

Here $g = MG/R_E^2$. Fig.1 sketches a dipole magnetic field line, a vertical for the radially, say outward pointing sum of electrical- and gravitational forces on sufficiently light test ions, and its direction along the magnetic field line. This parallel-B force changes sign passing the (magnetic) equator, λ=0, in such a way that if $\overline{qm_+}/(2e) - m > 0$ then the force gives rise to oscillatory motion of test ions along the magnetic field. Furthermore, the parallel force is varying with height for at least two reasons: First due to the variation of L, an effect which in each of our calculations for relatively local equatorial height regions will be considered small. Second due to the variations of $\overline{m}_+$ with height: When the fraction of heavy ion components decreases with increasing height, $\overline{m}_+$ will also decrease, and this effect may be non-negligible.

In our analytic calculations for equatorial regions λ will be assumed to be relatively small, so that an approximation for λ then is

$$\lambda = \frac{z}{LR_E} \tag{13}$$

where z is measured (positive or negative) along field lines from the equator. We note that the general formula for the relation between λ and z is

$$z = R_E L \int_0^{\lambda} \cos\lambda' \sqrt{1+3\sin^2\lambda'}\, d\lambda' . \tag{14}$$

Assuming small height variations, one obtains the approximation

$$F_{\parallel}^{E} = -\frac{2z}{LR_E}\left(\frac{\overline{qm_+}}{2e} - m\right)\frac{g}{L^2} \tag{15}$$

where now the dominant variation is due to variation in z . This force gives rise to harmonic oscillations with frequency

$$\omega = \omega_0^E = \sqrt{\frac{2g}{R_E L^3}\left(\frac{\overline{qm_+}}{2em} - 1\right)}. \tag{16}$$

The overestimated increase of the approximate force for relatively large z may to some extent be considered as a compensation for a neglect of an increase of $\overline{m}_+$ for large z, since large z corresponds to lower height.

For an O^+-electron background with $L\approx 1.2$ and z running from 3000km to 0 a test-helium ion (single ionized) has an approximate variation of 0.5eV of its kinetic energy due to the force Eq.(15). This variation is well above the background temperature normally found here [1]. A test proton will on the same background acquire nearly double of this energy running that distance.

2.2 Collisionless trapped particles characterized by $|v_{\parallel}| \ll |v_{\perp}|$ in equatorial magnetic mirror regions

The guiding centre motion of charged particles along the magnetic field is given from drift theory by

$$m\frac{dv_{\parallel}}{dt} = F_{\parallel}^{B} = -\mu\left(\frac{\partial B}{\partial \mathbf{r}}\right)_{\parallel}, \tag{17}$$

if other fields or interactions are neglected. Here μ is the (assumed adiabatic invariant) magnetic moment $mv_\perp^2 / 2B$. A straight forward calculation assuming a dipole magnetic field Eq.(9) gives the force $F_\parallel^B$,

$$F_\parallel^B = -\mu \frac{\mu_0}{4\pi} \frac{M_E}{r^4} \frac{3\sin\lambda(3+5\sin^2\lambda)}{(1+3\sin^2\lambda)}. \tag{18}$$

Particles characterised by $| v_\parallel | << | v_\perp |$ are easily trapped, [6]. Excursions of these particles away from the magnetic equator (λ=0) along the magnetic field may be considered small, and the above equation of motion may then be approximated by

$$m\frac{d^2z}{dt^2} = -\frac{9}{2}\frac{mv^2}{R_E L}\lambda = -\frac{9}{2}\frac{mv^2}{(R_E L)^2} z \tag{19}$$

where also v has been substituted for $v_\perp$ since $| v_\parallel | << | v_\perp |$. Solutions are harmonic with frequency

$$\omega = \omega_0^B = 3v / (\sqrt{2} L R_E). \tag{20}$$

Observe that this frequency depends on particle velocity, mainly the transverse velocity component.

2.3 Collisionless trapped particles characterised by $| v_\parallel | << | v_\perp |$ in combined gravity-, ambipolar- and magnetic mirror fields

From Eqs.(12) and (18) one obtains the combined force on strongly gyrating particles along a B-field line,

$$F_\parallel^{E,B} = F_\parallel^E + F_\parallel^B = \frac{\sin\lambda}{(1+3\sin^2\lambda)^{1/2}(1-\sin^2\lambda)^2} \left[-2\left(\frac{\overline{qm_+}}{2e} - m \right) \frac{g}{L^2} - \mu \frac{B(R_E L, 0)}{R_E L} \frac{3(3+5\sin^2\lambda)}{(1-\sin^2\lambda)^2(1+3\sin^2\lambda)^{1/2}} \right]. \tag{21}$$

Case (i): $\frac{\overline{qm_+}}{2e} - m > 0$ ("Ionospheric regions") when $| v_\parallel | << | v_\perp | \approx v$ for test particles

In "ionospheric" environments where $\frac{\overline{qm_+}}{2e} - m > 0$ $F_\parallel^{E,B}$ changes sign only through λ=0 and in such a way as to give rise to oscillations. For cases when $| v_\parallel | << | v_\perp |$ small oscillations are harmonic with frequency

$$\omega_0^{E,B} = \sqrt{(\omega_0^E)^2 + (\omega_0^B)^2}. \tag{22}$$

Case (ii): $\frac{\overline{qm_+}}{2e} - m < 0$ ("Outer-dipole regions") when $|v_{\|}| << |v_{\perp}| \approx v$ for test particles

If the background consists mainly of light ions (protons), then for He-test ions, say, $\overline{qm_+}/(2e) - m < 0$. Again assuming $|v_{\|}| << |v_{\perp}|$ we have for small λ, $\lambda \approx z/(R_E L)$, that

$$F_{\|}^{E,B} \approx \frac{z}{LR_E}\left[2(m - \frac{\overline{qm_+}}{2e})\frac{g}{L^2} - \frac{9}{2}\frac{mv^2}{R_E L}\right] \tag{23}$$

and the condition for harmonic oscillations around λ=0 in this case is

$$\frac{9}{2}\frac{mv^2}{R_E} > 2(m - \frac{\overline{qm_+}}{2e})\frac{g}{L} \tag{24}$$

which is fulfilled down to quite low $v_{\perp}$-velocity He-particles with energy of order 1eV. The frequency of oscillations becomes

$$\omega_{od}^{E,B} = \sqrt{\frac{9}{2}\frac{v^2}{(R_E L)^2} - 2(1 - \frac{\overline{qm_+}}{2me})\frac{g}{L^3 R_E}}. \tag{25}$$

which also depends on (mainly) transverse particle velocity.

2.4 Detrapping of collisionless particles characterised by $|v_{\|}| << |v_{\perp}|$ in combined gravity-, electric and magnetic mirror fields – and trapping in a double well potential

When still $\overline{qm_+}/(2e) - m < 0$, as in case (ii) above, and we consider particles with velocities obeying $|v_{\|}| << |v_{\perp}|$, an unstable equilibrium at the equator λ=0 may occur if the inequality Eq.(24) is turned around:

$$\frac{9}{2}\frac{mv^2}{R_E} < 2(m - \frac{\overline{qm_+}}{2e})\frac{g}{L}. \tag{26}$$

The fulfilment of this inequality for Earth conditions and relatively light particles requires transverse energies not higher than approximately 1eV. However, heavier ionized test particles stemming from a release may be warmer. Also, for more massive and larger planets, or even stars, of radius R_0, having a dipole-like magnetic field in some regions, the right hand side of the inequality Eq.(26) may increase by nearly two orders of magnitude and the left hand side decrease correspondingly, and hence the inequality may be fulfilled for a wide spectre of particle populations of relatively high transverse velocity. Anyway, when fulfilled a detrapping at λ=0 takes place. However, new stable equilibria will arise symmetrically on both sides (north- south) of the equator. These equilibria occur where the

forces $F_{\|}^{B}$ from Eq.(18) and $F_{\|}^{E}$ from Eq.(12) along the same B-field line balance, apart from the (unstable) balance at λ=0, say for $\lambda = \lambda_1$ given from

$$\frac{2(m-\overline{qm_+}/(2e))R_E g}{3\mu B(R_E L,0)L} = \frac{3+5\sin^2\lambda_1}{(1-\sin^2\lambda_1)^2(1+3\sin^2\lambda_1)^{1/2}}. \qquad (27)$$

For $-\pi/2 < \lambda < \pi/2$ only two solutions of λ exist. Along the magnetic field the test particles we consider then may move in a double-well potential. Using the z-coordinate along the magnetic field given from Eq.(13) instead of λ and assuming λ rather small, the resultant force $F^{E,B}$ may be approximated by

$$F_{\|}^{E,B}/m = \frac{z}{R_E L}\left(\frac{2g}{mL^2}(m-\frac{q\overline{m_+}}{2e}) - \frac{3\mu B(R_E L,0)}{mR_E L}\left(3+\frac{13}{2}\left(\frac{z}{R_E L}\right)^2\right)\right) \qquad (28)$$

giving the two stable points in the double well as

$$z = \pm R_E L\sqrt{2[2g(m-\frac{q\overline{m_+}}{2e})/(mL^2) - \frac{9\mu B(R_E L,0)}{mR_E L}]/(\frac{39\mu B(R_E L,0)}{mR_E L})}. \qquad (29)$$

A phase-plane plot of some solution curves of particle motion for variables and parameter choices such that Eq.(28) reads $F_{\|}^{E,B}/m = z(1-z^2)$ is shown in Fig.2. For low velocity and close to each of the stable points particles oscillate harmonically with frequency

$$\omega_0^{E,B} = \sqrt{2[2g(m-\frac{q\overline{m_+}}{2e})/(mL^2) - \frac{9\mu B(R_E L,0)}{mR_E L}]/(R_E L)}. \qquad (30)$$

3 A kinetic equation for trapped charged particles

3.1 Model kinetic equation including collisions for parallel-B evolution incorporating transverse-B drifting effects

We shall develop analytic solutions of a kinetic equation for a dilute component of ions that are trapped in parallel-B force fields like the ones described above. The dilute component of particles will be considered to stem from a source that in some of the modellings will be consistent with the assumption $|v_{\|}| << |v_{\perp}|$ also discussed above. Collisional effects between these particles and the relatively dense background particles will be taken into account using the special Fokker-Planck term in [7], see also [4], that may be generalised to the case of velocity anisotropy parallel and transverse to the magnetic field:

$$\left(\frac{\partial f}{\partial t}\right)_{F-P} = \beta_{\|}\frac{\partial}{\partial v_z}(v_z f) + q_{\|}\frac{\partial^2}{\partial v_z^2} f + \beta_{\perp}\frac{\partial}{\partial \mathbf{v}_{\perp}}\cdot(\mathbf{v}_{\perp} f) + q_{\perp}\frac{\partial^2}{\partial \mathbf{v}_{\perp}^2} f . \qquad (31)$$

Here $\beta_{\|}$ and $\beta_{\perp}$ are momentum transfer collision frequencies and $q_{\|}$ and $q_{\perp}$ collisional energy transfer coefficients between the dilute component and the background. We have $q_{\|} / \beta_{\|} = \kappa T_{0\|} / m$ and $q_{\perp} / \beta_{\perp} = \kappa T_{0\perp} / m$, where $T_{0\|}$ and $T_{0\perp}$, the parallel-B and transverse-B temperatures of the background, generally may be different. The term models a Brownian movement of test particles along and transverse to the magnetic field. One should observe that the rather simple collision term is linear and that it separates parallel-B and transverse-B processes, see the velocity moment equations below. In spite of this it has many of the characteristics of more detailed collision terms, and an advantage using this term is that analytic derivation of general solutions of the kinetic equation then is possible in some cases.

For the ionospheric example with the harmonic parallel-B ambipolar- and gravitational field component Eq.(15), the inclusion of collisions will not destroy an ambipolar trapping since the background temperature usually is quite low and will not excite test particles to reach atmospheric heights along magnetic field lines. For magnetic mirror regions in the "outer dipole region" the corresponding background temperature is considered to be higher, and what is more, the parallel-B trapping magnetic force in this case is proportional to the test particle's $v_{\perp}^2$ through the magnetic moment, and therefore in general will change when $v_{\perp}$ changes due to collisions. However, for some time the force field may be considered constant. To see this we may argument loosely as follows: In two-ions Coulomb interactions involving at least one quite high energy particle (in our modelling this could be a test ion or a background particle) the relative momentum and energy transfers in general are low: The velocity changes of test particles during such collisions, $\Delta\mathbf{v} = \Delta\mathbf{v}_{\perp} + \Delta\mathbf{v}_{\|}$, typically have contribution of the same order of magnitude both in the perpendicular- and parallel- magnetic field velocity directions, i.e. $|\Delta\mathbf{v}_{\perp}| \approx |\Delta\mathbf{v}_{\|}|$. In the modelling presented here the test particles (initially) obey $|v_{\|}| << |v_{\perp}|$. The parallel magnetic force on a test particle then changes as $|\Delta\mathbf{F}_{\|}| \approx |\mathbf{v}_{\perp}\Delta\mathbf{v}_{\perp}| \approx |\mathbf{v}_{\perp}\Delta\mathbf{v}_{\|}|$ during a collision and from Eq.(19) the change gives rise to an overall parallel velocity change in one oscillation period of order $|\mathbf{v}_{\|}||\Delta\mathbf{v}_{\|}| / |\mathbf{v}_{\perp}|$, hence much smaller than the change due to one collision, $\Delta\mathbf{v}_{\|}$. Therefore we may neglect the magnetic force change effect and conclude that particles that were initially trapped in a mirror magnetic field obeying $|v_{\|}| << |v_{\perp}|$, evolving on and colliding with an often relatively hot background, will continue for some time to move as if practically the mirror force field is constant. The same conclusion may be obtained for

magnetic mirrors in ionospheric regions for test particles obeying $|v_{\|}| << |v_{\perp}|$ if $v_{\perp}$ is large enough. For double wells $v_{\perp}$ can not be too large, cf. Eq.(26) and discussion there. Furthermore, when $v_{\perp}$ is large enough for test particles or the background is relatively warm, $|v_{\|}| << |v_{\perp}|$ may be expected to be valid for some time in spite of collisions and thus prevent particles from reaching atmospheric heights over a certain time span.

It will next be assumed the distribution function for the dilute component is almost symmetric in velocity transverse to the magnetic field, i.e. $f(\mathbf{v}) \approx f(v_z, v_{\perp}^2)$. An argument for doing this assumption is the short-period gyrations of particles in the magnetic field, say of order $10^{-3} s$ for protons and $B \approx 1$ gauss (much smaller than other time scales considered, see below) and the slow transverse-B drifts. We note once more that the collision term Eq.(31) separates parallel-B and transverse-B kinetic evolution, see also the moment equations below. Hence we may average out to "lowest order" transverse effects, and the kinetic equation may be simplified to an equation for only parallel-B variations. This simplification is expected to be better all the more particles gyrate in the magnetic field. Thus also global transverse-B effects are left out for a moment. Further below, however, transverse effects will be incorporated again to some extent. Hence, neglecting transverse-B position and velocity variations, we consider the distribution function $f(z, v_z, t)$ (of guiding centres) for the dilute component along the magnetic field (z-direction) to be given from the equation

$$\frac{\partial f}{\partial t} + v_z \frac{\partial f}{\partial z} + \frac{F_{\|}}{m} \frac{\partial f}{\partial v_z} = \beta(t) \frac{\partial}{\partial v_z}(v_z f) + q(t) \frac{\partial^2}{\partial v_z^2} f + S. \qquad (32)$$

Subscript "||"for β and q has been left out. $F_{\|}$ may for instance be equal $F_{\|}^{E}$ from Eq.(15) for the ionospheric case, or $F_{\|}^{B}$ from Eq.(18), averaged over transverse velocities for the case of magnetically trapped particles obeying $|v_{\|}| << |v_{\perp}|$, or $F_{\|}^{E,B}$ from Eq.(28) for the double-well potential case. For the two last cases the transverse averaging will introduce in $F_{\|}$ a transverse-B temperature dependency. In accordance with the discussion above this temperature may be considered almost constant. The collision parameters β and q are considered not to vary with z. However, we "bake" effects from equatiorial movements, say, and planet rotation left out above into the equation again by allowing for a time variation of the coefficients β and q reflecting variations of the background.

In Eq.(32) $S(z, v_z, t)$ is a source term. This term may in particular take simple forms as

$$S = M\tau(t) g(v_z) h(z) \qquad (33)$$

where M is a constant. Here $\tau(t)$ may take different forms, as the unit step function form $U(t) = \begin{cases} 1, & t > 0 \\ 0, & t \le 0 \end{cases}$, or, for an instantaneous source at $t = 0^+$, $\delta(t - 0^+)$. The functions g and h may also in particular take delta-function forms: A concentrated point source in phase-space (z, v_z) that is instantaneous and of amount M=1, i.e. when S has a form

$$S_\delta(z, v_z, t; z', v_z', s) = \delta(z - z')\delta(v - v_z')\delta(t - s) \tag{34}$$

gives rise to fundamental solutions f_δ which are of particular interest, both physically and mathematically.

It is clear that inhomogeneities for the ion distribution function are due to both the source-induced inhomogeneities and the inhomogeneity due to the forcing term.

We list some macroscopic equations for the parallel-B evolution. We may derive these from the "full" kinetic equation, i.e. before the transverse-B averaging above has been done, or from the transverse averaged Eq.(32). The collision term causes no coupling of parallel and transverse equations if no couplings have been incorporated in the collision parameters.

Starting from Eq.(32), defining $\langle \phi(v_z) \rangle = \int \phi(v_z) f dv_z / n$ where in particular $n = \int f dv_z$ is the density and $U_z = \int v_z f dv_z / n$ is the mean flow, we get the chain of equations

$$\begin{aligned}
&\frac{\partial}{\partial t} n + \frac{\partial}{\partial z}(nU_z) = S_{(1)} \\
&\frac{\partial}{\partial t} nmU_z + \frac{\partial}{\partial z}\left\langle nmv_z^2 \right\rangle - nF_\parallel = -nm\beta U_z + S_{(mv_z)} \\
&\frac{\partial}{\partial t}\left\langle nmv_z^2 / 2 \right\rangle + \frac{\partial}{\partial z}\left\langle nmv_z^3 / 2 \right\rangle - nF_\parallel U_z = -\beta\left\langle nmv_z^2 \right\rangle + qmn + S_{(mv_z^2/2)} \\
&\vdots
\end{aligned} \tag{35}\text{-}(37)$$

The subscripts on the source term contributions indicate the velocity moment performed. An alternative to this chain of equations we obtain defining the temperature T_z by $n\kappa T_z = \int m(v_z - U_z)^2 f dv_z$, and we then have instead

$$\begin{aligned}
&\frac{\partial}{\partial t} n + \frac{\partial}{\partial z}(nU_z) = S_{(1)} \\
&nm\left(\frac{\partial}{\partial t} U_z + U_z \frac{\partial}{\partial z} U_z\right) + \frac{\partial}{\partial z} n\kappa T_z - nF_\parallel = -nm\beta U_z + S_{(mv_z)} \\
&\frac{n\kappa}{2}\left(\frac{\partial}{\partial t} T_z + U_z \frac{\partial}{\partial z} T_z\right) + n\kappa T_z \frac{\partial U_z}{\partial z} + \frac{\partial q_z}{\partial z} = -n\kappa\beta(T_z - T_0) + S_{(m(v_z - U_z)^2/2)} \\
&\vdots
\end{aligned} \tag{38}\text{-}(40)$$

where

$$q_z(z,t) = \int \frac{1}{2} m (v_z - U_z)^3 f(z, v_z, t) dv_z \qquad (41)$$

is the heat transport and $T_0 = T_{0\|}$ is the background temperature. We observe that no transverse-B effects are picked up by the collision term in the averaging process. A more detailed collision term, say a Landau-Fokker-Planck term [8], generally would couple parallel- and transverse-B evolutions. However, using such a term, general analytic solutions of the kinetic equation can hardly be obtained.

3.2 Some estimates of parameter values in the collisional case.

We first give orders of magnitudes of collision related parameters in the kinetic equation for He^+- particles evolving on a low-temperature electron-O^+ background as in equatorial ionospheric regions. These (rather rough) estimates are based on more detailed collision terms than used in the present modelling. The thermal velocity for He^+-ions, the He^+-O^+ collision time (angle of order $\pi/2$ deflection time) and the associated effective mean free path for He^+-ions are (approximately), when isotropy in velocity space is assumed:

$$v_{thHe} \approx \frac{1}{2} 10^6 T_{He}^{1/2} \text{ cm/s}, \quad \tau_0 \approx 10^7 \frac{T_{He}^{3/2}}{\Lambda n_0} \text{ s}, \quad \lambda_{\text{He}} \approx \frac{1}{2} 10^{13} \frac{T_{He}^{2}}{\Lambda n_0} \text{ cm}. \qquad (42)$$

T_{He} is the He^+ ion temperature, measured in eV, n_0 is the background ion density (in $1/\text{cm}^3$), and Λ is the Coulomb-logarithm. If the He- ions are considered to have the same (low) temperature T_0 as the background particles, and we set this to 0.15 eV, and at the same time set the background density to 10^4 /cm^3, then, with Λ of order 10, we have

$$v_{thHe} \approx 10^5 \text{ cm/s}, \quad \tau_0 \approx 10 \text{ s}, \quad \lambda_{\text{He}} \approx 10^6 \text{ cm}. \qquad (43)$$

We next compare the collision frequency $1/\tau_0$ with

$$\omega_0^E = \sqrt{\frac{2g}{R_E L^3}\left(\frac{\overline{qm_+}}{2em} - 1\right)} \text{ and } \omega_0^B = \frac{3\nu}{\sqrt{2} L R_E}. \qquad (44)$$

For He^+-ions on a dominant O^+-ion background ω_0^E reduces to $\omega_0^E = \sqrt{\frac{2}{R_E L^3} g}$, which for Earth (and $L \approx 1$) gives $\omega_0^E \approx 1.7\ 10^{-3}\ /\ s$. This is rather small, as compared to the collision frequency $1/\tau_0$ above. However, for H^+-ions on the same background ω_0^E would increase by a factor $\sqrt{7}$. There is also an increase for multiple ionized test particles. For more dilute

backgrounds rather high up, say of densities 10^3-10^2 /cm^3, or because of less effective collisions for some reason, for instance if test particles are highly anisotropic with $|v_{\parallel}| << |v_{\perp}|$ such that, say $T_{\perp} >> 0.15$ eV, the collision frequency could be drastically reduced and be comparable with, or even less than, ω_0^E. The conclusion is that considering various orderings between say ω_0^E and $1/\tau_0$, from oscillation dominated ($\omega_0^E > 1/\tau_0$) to collision dominated ($\omega_0^E < 1/\tau_0$) may be of more than academic interest in ambipolar trapping of test particles in higher equatorial ionospheric regions. ω_0^B, on the other hand, is of order $10^{-3} T_{He\perp}{}^{1/2} L^{-1}$ / s for a thermal He-ion where $T_{He\perp}$ again is measured in eV. As $T_{He\perp}$ increases ω_0^B also increases while the collision frequency decreases. Hence it may be highly relevant to consider a wide spectre of relative magnitudes between these frequencies. This may also be said for the combined magnetic mirror and ambipolar field wells discussed above.

4 Solution of the test particle kinetic equation in the collisionless case

4.1 Harmonic well potential

We here solve Eq.(32) for a harmonic well force field, neglecting collisional effects and assuming an instantaneous source at time $t = 0^+$, i.e. we solve

$$\frac{\partial f}{\partial t} + v_z \frac{\partial f}{\partial z} - \omega^2 z \frac{\partial f}{\partial v_z} = Mg(v_z)h(z)\delta(t - 0^+). \tag{45}$$

ω is assumed constant. It may in particular be given from Eqs.(16), (20), (22) or (25). We shall use the initial condition

$$f(z, v_z, 0) = 0. \tag{46}$$

New variables instead of (z, v_z) are introduced by solving the set of characteristic equations

$$\begin{aligned} \frac{dv_z}{dt} &= -\omega^2 z \\ \frac{dz}{dt} &= v_z \end{aligned} \tag{47}$$

Writing the solution of Eq.(47) as

$$\begin{aligned} z &= c_1 \cos \omega t + c_2 \sin \omega t \\ v_z &= -\omega c_1 \sin \omega t + \omega c_2 \cos \omega t \end{aligned} \tag{48}$$

the new variables (c,ζ) are obtained by solving for c_1 and c_2, hence

$$c = z\cos\omega t - \frac{v_z}{\omega}\sin\omega t$$
$$\zeta = z\sin\omega t + \frac{v_z}{\omega}\cos\omega t \qquad (49)$$

f in these new variables, $F(c,\zeta,t)$, then obeys the equation

$$\frac{\partial F}{\partial t} = Mg(-\omega c\sin\omega t + \omega\zeta\cos\omega t)h(c\cos\omega t + \zeta\sin\omega t)\delta(t-0^+) \qquad (50)$$

which may be readily integrated to give

$$F = Mg(\omega\zeta)h(c) \qquad (51)$$

and for f,

$$f(z,v_z,t) = Mg(v_z\cos\omega t + \omega z\sin\omega t)h(z\cos\omega t - \frac{v_z}{\omega}\sin\omega t). \qquad (52)$$

Fig.3 shows $f(z,v_z,t)$ for various times when M=1 and we let $g(v_z)h(z) = \exp(-v_z^2-(z-1)^2)/\pi$ and $\omega = 1$ using a relevant set of scales for the dimensionless z, v_z and t. The distribution function is seen to move without distortion periodically in the phase-plane.

4.2 Double well potential

We consider now the equation

$$\frac{\partial f}{\partial t} + v_z\frac{\partial f}{\partial z} + \frac{F_{\|}}{m}\frac{\partial f}{\partial v_z} = Mg(v_z)h(z)\delta(t-0^+) \qquad (53)$$

where $F_{\|}$ may be given approximately from Eq.(28),

$$F_{\|}^{E,B}/m = \frac{z}{R_E L}\left(\alpha_1 - \alpha_2(3+13/2\cdot\left(\frac{z}{R_E L}\right)^2)\right) \qquad (54)$$

and where

$$\alpha_1 = \frac{2g}{mL^2}(m - \frac{q\overline{m_+}}{2e})$$
$$\alpha_2 = \frac{3\langle\mu\rangle B(R_E L,0)}{mR_E L} \qquad (55)$$

both are considered constant and fulfilling $3\alpha_2 < \alpha_1$ (cf. also the transverse averaging discussed above). The characteristic equations

$$\frac{dv_z}{dt} = \frac{z}{R_E L}\left(\alpha_1 - \alpha_2(3+13/2\cdot\left(\frac{z}{R_E L}\right)^2)\right)$$
$$\frac{dz}{dt} = v_z \tag{56}$$

now are non-linear, and we express formally the solutions using a streaming operator S_{-t}, [9] ,which transforms phase-space coordinates backward in time according to the equations of motion:

$$z(-t) = S_{-t}z$$
$$v_z(-t) = S_{-t}v_z \tag{57}$$

where (z, v_z) are corresponding coordinates at t=0. The solution of Eq.(53) may then be formally expressed as

$$f(z, v_z, t) = MS_{-t}g(v_z)h(z) = Mg(S_{-t}v_z)h(S_{-t}z). \tag{58}$$

Fig.4 shows the solution at various times when $g(v_z)h(z) = \exp(-v_z^2 - z^2)/\pi$ and M=1 using again a relevant set of scales for the dimensionless z, v_z and t. We consider in particular $\alpha_1 = 19/13$ and $\alpha_2 = 2/13$ thereby placing the well-centres at z=±1.

5 Solution of test particle kinetic equation when collisions are included

5.1 Harmonic well potential and shifting background

In the case of a harmonic well force field we put Eq.(32) on the form

$$\frac{\partial f}{\partial t} + v_z\frac{\partial f}{\partial z} - \left(\omega^2 z + \beta(\varepsilon t)v_z\right)\frac{\partial f}{\partial v_z} = \beta(\varepsilon t)f + q(t)\frac{\partial^2}{\partial v_z^2}f + S \tag{59}$$

assumed valid for $t > 0$, $-\infty < z < \infty$, $-\infty < v_z < \infty$ on relevant scales, with source given in this domain. We have allowed for time variations (assumed known) of the parameters β and q. The variation of β is assumed slow (ε<<1). These variations may reflect effects of shifting background as day-night effects. We assume also here that ω is constant: ω from both Eq.(16) and Eq.(20) are rather constant. Again we set $f(z, v_z, 0) = 0$.

Along the same lines as above, new variables (c,ζ) instead of (z,v_z) are first introduced by solving the set of characteristic equations, which now are

$$\frac{dv_z}{dt} = -(\omega^2 z + \beta(\varepsilon t)v_z)$$
$$\frac{dz}{dt} = v_z \tag{60}$$

or,

$$\frac{d^2z}{dt^2} + \beta(\varepsilon t)\frac{dz}{dt} + \omega^2 z = 0$$
$$v_z = \frac{dz}{dt} \tag{61}$$

Eq.(61) may be solved by standard perturbation techniques, [10], and we obtain to lowest order in ε,

$$z = c_2 A_0(\varepsilon t)e^{\theta_1} - c_1 B_0(\varepsilon t)e^{\theta_2}$$
$$v_z = c_2 r_1(\varepsilon t)A_0(\varepsilon t)e^{\theta_1} - c_1 r_2(\varepsilon t)B_0(\varepsilon t)e^{\theta_2} \tag{62}$$

where r_i, i=1,2, are slowly time-varying roots of the characteristic equation

$$r^2 + \beta(\varepsilon t)r + \omega^2 = 0 \tag{63}$$

and

$$A_0(\varepsilon t) = \exp(-\int_0^{\varepsilon t} \frac{r_1'(\xi)d\xi}{2r_1(\xi) + \beta(\xi)})$$
$$B_0(\varepsilon t) = \exp(-\int_0^{\varepsilon t} \frac{r_2'(\xi)d\xi}{2r_2(\xi) + \beta(\xi)}) \tag{64}$$

θ_1 and θ_2 are solution of

$$\frac{d\theta_1}{dt} = r_1(\varepsilon t)$$
$$\frac{d\theta_2}{dt} = r_2(\varepsilon t) \tag{65}$$

i.e.,

$$\theta_1(t, \varepsilon t) = \int_0^t r_1(\varepsilon s)ds$$
$$\theta_2(t, \varepsilon t) = \int_0^t r_2(\varepsilon s)ds \tag{66}$$

We solve Eq.(62) for c_1 and c_2 and take these expressions as the definition of the new variables, hence:

$$c = \frac{v_z - r_1 z}{B_0 e^{\theta_2}(r_1 - r_2)}$$
$$\zeta = \frac{v_z - r_2 z}{A_0 e^{\theta_1}(r_1 - r_2)} \quad . \tag{67}$$

The inverse transformation returns the original variables:

$$z = \zeta A_0 e^{\theta_1} - c B_0 e^{\theta_2}$$
$$v_z = r_1 \zeta A_0 e^{\theta_1} - r_2 c B_0 e^{\theta_2} \quad . \tag{68}$$

For the case that both roots r_1 and r_2 are real, all quantities above are real, in particular the variables c and ζ. For the case that the roots are complex conjugates, one observes that

$$\bar{B}_0 = A_0 \ , \ \bar{\theta}_2 = \theta_1 \tag{69}$$

and new variables c' and ζ' defined by

$$c' = \zeta - c$$
$$\zeta' = i(c + \zeta) \tag{70}$$

which also are real, could be used instead. However, we first solve the Eq.(59) for the real root case, and comment later on the slight modifications that must be adopted to extend the solution to cover the complex conjugate root case.

5.1.1 Real root case

Using the variables c and ζ the distribution function $f(z, v_z, t)$ transforms to $F(c, \zeta, t)$ which to lowest order in ε obeys the equation

$$\frac{\partial F}{\partial t} - \beta F = q(t)\left(\left(\frac{1}{B_0 e^{\theta_2}(r_1 - r_2)}\right)^2 \frac{\partial^2 F}{\partial c^2} + 2\frac{1}{A_0 B_0 e^{\theta_1 + \theta_2}(r_1 - r_2)^2} \frac{\partial^2 F}{\partial c \partial \zeta} + \left(\frac{1}{A_0 e^{\theta_1}(r_1 - r_2)}\right)^2 \frac{\partial^2 F}{\partial \zeta^2} \right)$$
$$+ S(c, \zeta, t) \tag{71}$$

with transformed source term S'. Introducing

$$W = F e^{-\int_0^t \beta(\varepsilon\tau) d\tau} \tag{72}$$

we have the equation for W,

$$\frac{\partial W}{\partial t} = q(t)\left(\left(\frac{1}{B_0 e^{\theta_2}(r_1 - r_2)}\right)^2 \frac{\partial^2 W}{\partial c^2} + 2\frac{1}{A_0 B_0 e^{\theta_1 + \theta_2}(r_1 - r_2)^2} \frac{\partial^2 W}{\partial c \partial \zeta} + \left(\frac{1}{A_0 e^{\theta_1}(r_1 - r_2)}\right)^2 \frac{\partial^2 W}{\partial \zeta^2} \right)$$
$$+ S'(c, \zeta, t) \tag{73}$$

where the source term S' is

$$S'(c, \zeta, t) = S(c, \zeta, t) e^{-\int_0^t \beta(\varepsilon\tau) d\tau} \quad . \tag{74}$$

Eq.(73) may be solved by Fourier transformation. Denoting the transformed of W by

$$W_{k_1k_2}(t) = \frac{1}{2\pi}\int_{-\infty}^{+\infty} d\zeta \int_{-\infty}^{+\infty} dc W(c,\zeta,t) e^{ik_1 c} e^{ik_2 \zeta}, \tag{75}$$

the transformed equation becomes

$$\frac{\partial W_{k_1k_2}}{\partial t} + q(t)\left(\frac{e^{-2\theta_2}}{B_0{}^2 (r_1 - r_2)^2} k_1{}^2 + 2\frac{e^{-\theta_1-\theta_2}}{A_0 B_0 (r_1 - r_2)^2} k_1 k_2 + \frac{e^{-2\theta_1}}{A_0{}^2 (r_1 - r_2)^2} k_2{}^2 \right) W_{k_1k_2} = S''_{k_1k_2}(t) \tag{76}$$

where

$$S'_{k_1k_2}(t) = \frac{1}{2\pi}\int_{-\infty}^{+\infty} d\zeta \int_{-\infty}^{+\infty} dc S'(c,\zeta,t) e^{ik_1 c} e^{ik_2 \zeta} \ . \tag{77}$$

Eq.(76) may be readily integrated,

$$W_{k_1k_2}(t) = \int_0^t ds' \, S''_{k_1k_2}(s') \exp\left(-\int_{s'}^t d\tau \left(\frac{e^{-2\theta_2(\tau)} q(\tau)}{B_0{}^2(\varepsilon\tau)(r_1(\varepsilon\tau) - r_2(\varepsilon\tau))^2} k_1{}^2 + \right.\right.$$

$$\left.\left. 2\frac{e^{-\theta_1(\tau)-\theta_2(\tau)} q(\tau)}{A_0(\varepsilon\tau) B_0(\varepsilon\tau)(r_1(\varepsilon\tau) - r_2(\varepsilon\tau))^2} k_1 k_2 + \frac{e^{-2\theta_1(\tau)} q(\tau)}{A_0{}^2(\varepsilon\tau)(r_1(\varepsilon\tau) - r_2(\varepsilon\tau))^2} k_2{}^2 \right)\right). \tag{78}$$

$W(c,\zeta,t)$ is then given by inverse Fourier transformation

$$W(c,\zeta,t) = \frac{1}{2\pi}\int_{-\infty}^{+\infty} dk_1 \int_{-\infty}^{+\infty} dk_2 W_{k_1k_2}(t) e^{-ik_1 c} e^{-ik_2 \zeta} \tag{79}$$

and from Eqs.(72) and (67) eventually $F(c,\zeta,t)$ and $f(z,v_z,t)$ are obtained.
However, we may build up the solution from fundamental solutions, and therefore we now seek an explicit form of f_δ.

5.1.1.1 Fundamental solutions due to instantaneous point sources.

We here derive the fundamental solution for the case with an instantaneous point source at (z', v_z') at time s of amount M=1

$$S_\delta(z,v_z,t) = \delta(z - z')\delta(v_z - v_z')\delta(t - s) \tag{80}$$

which in the new variables transforms into

$$S'_\delta(c,\zeta,t) = \delta(\zeta A_0(\varepsilon t) e^{\theta_1(t)} - cB_0(\varepsilon t) e^{\theta_2(t)} - z')\delta(r_1(\varepsilon t)\zeta A_0(\varepsilon t) e^{\theta_1(t)} - r_2(\varepsilon t) cB_0(\varepsilon t) e^{\theta_2(t)} - v_z')\delta(t - s) \tag{81}$$

or, after some rewritings, to

$$S_\delta'(c,\zeta,t) = \frac{1}{|\, r_1(\varepsilon s) - r_2(\varepsilon s)\,|} \frac{1}{|\, A_0(\varepsilon s) B_0(\varepsilon s) e^{\theta_1(s)+\theta_2(s)}\,|} \delta(c + c^*)\delta(\zeta + \zeta^*)\delta(t - s) \tag{82}$$

where

$$c^* = \frac{1}{B_0(\varepsilon s)e^{\theta_2(s)}} \frac{r_1(\varepsilon s)z' - v_z'}{r_1(\varepsilon s) - r_2(\varepsilon s)} \quad , \quad \zeta^* = \frac{1}{A_0(\varepsilon s)e^{\theta_1(s)}} \frac{r_2(\varepsilon s)z' - v_z'}{r_1(\varepsilon s) - r_2(\varepsilon s)}. \tag{83}$$

The transformed of the source term Eq.(82) then is

$$S''_{\delta,k_1k_2}(t) = \frac{1}{2\pi} \frac{e^{-\int_0^s \beta(\varepsilon\tau)d\tau}}{|r_1(\varepsilon s) - r_2(\varepsilon s)|} \frac{1}{|A_0(\varepsilon s)B_0(\varepsilon s)e^{\theta_1(s)+\theta_2(s)}|} e^{-ik_1c^*} e^{-ik_2\zeta^*} \delta(t-s) \tag{84}$$

to be substituted for $S''_{k_1k_2}$ into the expression for $W_{k_1k_2}$, Eq.(78). Inverse Fourier transformation then returns $W_\delta(c,\zeta,t)$, and from Eq.(72) we have F_δ and eventually f_δ:

$$f_\delta(z.v_z,t;z',v_z',s) = \frac{1}{(2\pi)^2} \frac{e^{\int_s^t \beta(\varepsilon\tau)d\tau}}{|r_1(\varepsilon s) - r_2(\varepsilon s)|} \frac{1}{|A_0(\varepsilon s)B_0(\varepsilon s)e^{\theta_1(s)+\theta_2(s)}|} \int_{-\infty}^{+\infty} dk_1 \int_{-\infty}^{+\infty} dk_2 e^{-ik_1(c+c^*)} e^{-ik_2(\zeta+\zeta^*)} \exp(-\int_s^t d\tau$$

$$\frac{1}{(r_1(\varepsilon\tau) - r_2(\varepsilon\tau))^2} \left(\frac{e^{-2\theta_2(\tau)}q(\tau)}{B_0{}^2(\varepsilon\tau)} k_1{}^2 + 2\frac{e^{-\theta_1(\tau)-\theta_2(\tau)}q(\tau)}{A_0(\varepsilon\tau)B_0(\varepsilon\tau)} k_1k_2 + \frac{e^{-2\theta_1(\tau)}q(\tau)}{A_0{}^2(\varepsilon\tau)} k_2{}^2 \right)). \tag{85}$$

The *k*-integrations can both be performed, and we get,

$$f_\delta(z.v_z,t;z',v_z',s) = \frac{1}{4\pi} \frac{e^{\int_s^t \beta(\varepsilon\tau)d\tau}}{|r_1(\varepsilon s) - r_2(\varepsilon s)|} \frac{1}{|A_0(\varepsilon s)B_0(\varepsilon s)e^{\theta_1(s)+\theta_2(s)}|} \frac{1}{\sqrt{ad-b^2}} \exp(-\frac{dZ^2 + aC^2 - 2bCZ}{4(ad-b^2)}) \tag{86}$$

We have here introduced

$$\begin{aligned} a(t) &= \int_s^t d\tau \frac{q(\tau)}{(r_1(\varepsilon\tau) - r_2(\varepsilon\tau))^2} \frac{e^{-2\theta_1(\tau)}}{A_0(\varepsilon\tau)^2} \\ b(t) &= \int_s^t d\tau \frac{q(\tau)}{(r_1(\varepsilon\tau) - r_2(\varepsilon\tau))^2} \frac{e^{-(\theta_1(\tau)+\theta_2(\tau))}}{A_0(\varepsilon\tau)B_0(\varepsilon\tau)} \\ d(t) &= \int_s^t d\tau \frac{q(\tau)}{(r_1(\varepsilon\tau) - r_2(\varepsilon\tau))^2} \frac{e^{-2\theta_2(\tau)}}{B_0(\varepsilon\tau)^2} \end{aligned} \tag{87}$$

and

$$\begin{aligned} C = c + c^* &= \frac{v_z - r_1(\varepsilon t)z}{B_0(\varepsilon t)e^{\theta_2(t)}(r_1(\varepsilon t) - r_2(\varepsilon t))} - \frac{v_z' - r_1(\varepsilon s)z'}{B_0(\varepsilon s)e^{\theta_2(s)}(r_1(\varepsilon s) - r_2(\varepsilon s))} \\ Z = \zeta + \zeta^* &= \frac{v_z - r_2(\varepsilon t)z}{A_0(\varepsilon t)e^{\theta_1(t)}(r_1(\varepsilon t) - r_2(\varepsilon t))} - \frac{v_z' - r_2(\varepsilon s)z'}{A_0(\varepsilon s)e^{\theta_1(s)}(r_1(\varepsilon s) - r_2(\varepsilon s))} \end{aligned} . \tag{88}$$

Observe that (since roots r_1 and r_2 were assumed real) all of $a(t)$, $b(t)$ and $d(t)$ are positive, and that $ad-b^2 > 0$.

5.1.1.2 Solution due to a general source.

A solution that obeys $f(z,v_z,t=0)=0$ and is due to a source $S(z,v_z,t)$ for $t>0, -\infty < z < \infty, -\infty < v_z < \infty$ may be written as

$$f(z,v_z,t)=\int_0^t ds\int_{-\infty}^{\infty} dz'\int_{-\infty}^{\infty} dv_z' f_\delta(z,v_z,t;z',v_z',s)S(z',v_z',s) \tag{89}$$

where f_δ is given from Eq.(86). This may for instance be seen by direct substitution using that (in the limit $s\to t^-$)

$$f_\delta(z,v_z,t;z',v_z',t)=\delta(z-z')\delta(v_z-v_z'). \tag{90}$$

5.1.2 Case of complex conjugate roots

In contrast to the case $\beta(\varepsilon t)^2-4\omega^2>0$, when both roots r_1 and r_2 are real (and negative),

$$r_1(\varepsilon t)=\frac{-\beta(\varepsilon t)+\sqrt{\beta(\varepsilon t)^2-4\omega^2}}{2}\ ,\ r_2(\varepsilon t)=\frac{-\beta(\varepsilon t)-\sqrt{\beta(\varepsilon t)^2-4\omega^2}}{2}\ , \tag{91}$$

and damping is characteristic, the case $\beta(\varepsilon t)^2-4\omega^2<0$ gives rise to complex conjugate roots,

$$r_1(\varepsilon t)=\frac{-\beta(\varepsilon t)+i\sqrt{4\omega^2-\beta(\varepsilon t)^2}}{2}\ ,\ r_2(\varepsilon t)=\frac{-\beta(\varepsilon t)-i\sqrt{4\omega^2-\beta(\varepsilon t)^2}}{2} \tag{92}$$

and also oscillation becomes characteristic. In this case the solution procedure as in the real root case may be repeated using instead the variables (c',ζ') from Eq.(70). The results are similar to the above real-root forms. However, these forms, and f_δ in particular, may be obtained from Eq.(86), observing the following: Because of Eq.(92)

$$\overline{C}=-Z \tag{93}$$

from Eq.(88). Furthermore then

$$\begin{aligned}\overline{d}&=a\\ \overline{b}&=b\end{aligned} \tag{94}$$

and hence $ad-b^2$ is real (but turns negative).Then f_δ from Eq.(86) turns into

$$f_\delta(z.v_z,t;z',v_z',s)=\frac{1}{4\pi}\frac{e^{\int_s^t\beta(\varepsilon\tau)d\tau}}{|\,r_1(\varepsilon s)-r_2(\varepsilon s)\,||\,A_0(\varepsilon s)e^{\theta_1(s)}\,|^2}\frac{1}{\sqrt{|\,(ad-b^2)\,|}}\exp\left(-\frac{2\,\mathrm{Re}(dZ^2)+2b\,|\,C^2\,|}{4(ad-b^2)}\right) \tag{95}$$

where |.| now denotes absolute value.

5.2 Harmonic well potential, shifting background and oscillating field

We here shortly note the changes to be made in the solutions Eqs.(86) and (95) when we also include an oscillating field in the modelling and thereby mimic some additional effects on the test particle modelling above. More specifically, we solve

$$\frac{\partial f}{\partial t}+v_z\frac{\partial f}{\partial z}-\left(\omega^2 z+\frac{F_0\cos\omega_0 t}{m}+\beta(\varepsilon t)v_z\right)\frac{\partial f}{\partial v_z}=\beta(\varepsilon t)f+q(t)\frac{\partial^2}{\partial v_z^2}f+S. \tag{96}$$

We assume that both F_0 and ω_0 are real constants. As before the solution of the characteristic equations

$$\begin{aligned}\frac{dv_z}{dt}&=-(\omega^2 z+\beta(\varepsilon t)v_z+\frac{F_0\cos\omega_0 t}{m})\\ \frac{dz}{dt}&=v_z\end{aligned} \tag{97}$$

gives a set of new variables which we denote by (c'',ζ'') to replace (c,ζ) from Eq.(67). We get,

$$\begin{aligned}c''&=\frac{v_z-v_p(t)-r_1(z-z_p(t))}{B_0e^{\theta_2}(r_1-r_2)}\\ \zeta''&=\frac{v_z-v_p(t)-r_2(z-z_p(t))}{A_0e^{\theta_1}(r_1-r_2)}\end{aligned} \tag{98}$$

and for (z,v_z),

$$\begin{aligned}z&=\zeta''A_0e^{\theta_1}-c''B_0e^{\theta_2}+z_p(t)\\ v_z&=r_1\zeta''A_0e^{\theta_1}-r_2c''B_0e^{\theta_2}+v_p(t)\end{aligned}. \tag{99}$$

Here $v_p(t)=\frac{dz_p(t)}{dt}$, and $(z_p(t),v_p(t))$ is a particular solution of the characteristic equations Eq.(97), which now are inhomogeneous in contrast to the homogeneous characteristic equations Eq.(60). To lowest order,

$$\begin{aligned}z_p(t)&=-\frac{F_0}{m}\frac{1}{\left(\omega^2-\omega_0^2\right)^2+\beta^2(\varepsilon t)\omega_0^2}\left((\omega^2-\omega_0^2)\cos\omega_0 t+\beta(\varepsilon t)\omega_0\sin\omega_0 t\right)\\ v_p(t)&=\frac{F_0}{m}\frac{\omega_0}{\left(\omega^2-\omega_0^2\right)^2+\beta^2(\varepsilon t)\omega_0^2}\left((\omega^2-\omega_0^2)\sin\omega_0 t-\beta(\varepsilon t)\omega_0\cos\omega_0 t\right)\end{aligned}. \tag{100}$$

The procedure to solve the kinetic equation is the same as in the forgoing section, and it readily can be shown that the solutions of the kinetic equation, Eq.(96), both in the real root- and the complex conjugate root-case discussed earlier, assuming an instantaneous point source, Eq.(80), still are of the forms Eq.(86) and Eq.(95). The only changes to be made are that C and Z from Eq.(88) transform to

$$\begin{aligned}C&\to\frac{v_z-v_p(t)-r_1(\varepsilon t)(z-z_p(t))}{B_0(\varepsilon t)e^{\theta_2(t)}(r_1(\varepsilon t)-r_2(\varepsilon t))}-\frac{v_z'-v_p(s)-r_1(\varepsilon s)(z'-z_p(s))}{B_0(\varepsilon s)e^{\theta_2(s)}(r_1(\varepsilon s)-r_2(\varepsilon s))}\\ Z&\to\frac{v_z-v_p(t)-r_2(\varepsilon t)(z-z_p(t))}{A_0(\varepsilon t)e^{\theta_1(t)}(r_1(\varepsilon t)-r_2(\varepsilon t))}-\frac{v_z'-v_p(s)-r_2(\varepsilon s)(z'-z_p(s))}{A_0(\varepsilon s)e^{\theta_1(s)}(r_1(\varepsilon s)-r_2(\varepsilon s))}\end{aligned}. \tag{101}$$

All of r_1, r_2, A_0, B_0, θ_1, and θ_2 are as above.

Figs.5 and 6 illustrate some fundamental solutions at various times for two cases. In both cases the time-variations of parameters may reflect variation in the background. We note that variables are dimensionless using scales that are relevant in particular cases, the intention being both to simplify and to stress more on the relative orderings of effects that come into play. Fig.5 includes collisional friction and diffusion that slowly decay in time, plus the effect of a time-oscillating field. The effects of decreasing the friction alone from the start, or increasing the background temperature alone from the start, are shown at time t=20. One may observe that due to the decaying collision effect the distribution soon follows an almost collisionless evolution. In Fig.6 we illustrate an evolution where the friction is held rather large and constant ($\beta(t) \equiv 1$) while the background temperature varies periodically: $q(t)$ varies stepwise between 0.25 and 0.05 with a period equal to 10. Hence the distribution function eventually shows a "breathing" behaviour between a wide (warm) state and a peaked (cold) state that may go on for some time. The same rather weak time-oscillating field is included, but due to the higher friction the centre of the distribution nearly settles around (0,0) in phase-space.

5.3 Double well potential and oscillating field- strange attractors

We consider in this section the equation

$$\frac{\partial f}{\partial t} + v_z \frac{\partial f}{\partial z} + \frac{F_{//}^{E,B}}{m} \frac{\partial f}{\partial v_z} = \beta \frac{\partial}{\partial v_z}(v_z f) + \frac{F_0 \cos(\omega_0 t)}{m} \frac{\partial f}{\partial v_z} + Mg(v_z)h(z)\delta(t-0^+) \qquad (102)$$

which includes the double well force, Eq.(28) or (54), the momentum collisional transfer term, and, instead of the collisional velocity diffusion term, a time-oscillating forcing term, besides a source term. We do not take into account space dependency in the additional forcing. The neglect of the collisional velocity diffusion term may for instance be due to a very low parallel-B background temperature $T_{0//}$ ($q / \beta = \kappa T_{0//} / m \approx 0$), for instance in a transition-stage from a collisional state to a collisionless state where the diffusion effect first dies away. Hence friction and cool-down of test particles may be the main collisional effects left, at least for part of the evolution, see below. Adding a parallel-B oscillating forcing term will excite test particles and in some way counter-balance the energy dissipation. However, energy from a pure time-oscillating field goes into ordered motion as far as Eqs.(38)-(40) give an adequate description.

The equation is cast into the form

$$\frac{\partial f}{\partial t} + v_z \frac{\partial f}{\partial z} + \left(\frac{F_{//}^{E,B}}{m} - \frac{F_0 \cos(\omega_0 t)}{m} - \beta(t) v_z \right) \frac{\partial f}{\partial v_z} = \beta(t) f + Mg(v_z)h(z)\delta(t-0^+) \qquad (103)$$

Multiplying by $e^{-\int_0^t \beta(s)ds}$ and letting $W = e^{-\int_0^t \beta(s)ds} f$ we have for W the equation

$$\frac{\partial W}{\partial t} + v_z \frac{\partial W}{\partial z} + \left(\frac{F_{//}^{E,B}}{m} - \frac{F_0 \cos(\omega_0 t)}{m} - \beta(t) v_z \right) \frac{\partial W}{\partial v_z} = Mg(v_z)h(z)\delta(t - 0^+). \quad (104)$$

The corresponding characteristic equations now are

$$\begin{aligned} \frac{dz}{dt} &= v_z \\ \frac{dv_z}{dt} &= \frac{F_{//}^{E,B}}{m} - \frac{F_0 \cos(\omega_0 t)}{m} - \beta(t) v_z \end{aligned} \quad (105)$$

We may write the solution of f formally as

$$f(z, v_z, t) = Me^{\int_0^t \beta(s)ds} g(v_z(-t))h(z(-t)). \quad (106)$$

where $z(-t), v_z(-t)$ are the unique position and velocity at time $-t$ according to Eqs.(105), given that they are z, v_z at time t=0.

Depending on the actual condition, there are several, if not infinite, choices of parameter values that may be (more or less) relevant to use in solution-studies. These choices may include cases that lead to solutions of Eq.(105) that have strange attractors. In the illustrations that follow we have made such a particular choice of parameters. Note, however, that in our solution procedure leading to Eq.(106), a backward-in-time transformation is used.

Fig.7 shows solutions without an oscillating forcing term ($F_0 = 0$) for various times using the same parameter values for α_1 and α_2 and the g- and h- functions as in Fig.4, i.e. $\alpha_1 = 19/13$ and $\alpha_2 = 2/13$ and $g(v_z)h(z) = \exp(-v_z^2 - z^2)/\pi$, M=1, plus the constant friction $\beta(t) \equiv 0.25$. Variables are dimensionless using relevant scales. As compared to Fig.4 one observes the peaked distribution that develops reflecting the contraction of phase-space volume of particles and conservation of particle number. In Figs.8-9 we have added forcing, using $F_0 / m = 0.4$ and $\omega_0 = 1$, leaving other parameters as on the forgoing figure: In Fig.8 we have used $g(v_z)h(z) = \exp(-v_z^2 - z^2)/\pi$ and in Fig.9 $g(v_z)h(z) = \exp(-v_z^2 - (z+1)^2)/\pi$, i.e. we have successively placed the centre of the source at z=0 and z=–1, i.e. at two of the equilibrium positions of the well. The choices for the well-parameters, the strength of the oscillating forcing term and its frequency and the friction term now coincide with known choices from particle dynamic theory that lead to solutions with strange attractors as time goes on, [11], [12]. In our development solving a particular kinetic equation, patterns that look like cross sections of strange attractors in short

time seem to develop as support for the distribution function in phase-space. In Fig.8 some blow-ups at $t=8\pi$ show fractal similarities.

Though solutions in general are parameter dependent, the examples given may indicate that the combined effects incorporated in Eq.(102) may in some cases lead to peculiar particle distribution functions. However, as a rule the neglect of the velocity diffusion term is an approximation that ceases to be valid as spikes and strong velocity gradients develop, and some sort of balance may be expected when the effect is included. In this balance the spikes that have got time to develop may for some time "live" further on individually in phase space (with similar local velocity spreads), since the modelling kinetic equation is linear and hence has no non-linear couplings incorporated. In Fig.10 we have let the friction coefficient be time-dependent and decaying as $\beta(t) = 0.25e^{-0.2t}$, and we show solutions for $t=2\pi$ and $t=8\pi$ when other parameters and the choice of initial distribution are as in Fig.8. Spikes develop that to some extent "freeze", since the distribution function soon goes into a nearly collisionless evolution.

6 Summary and conclusion

Various evolutions of dilute ion populations, evolving on plasma backgrounds in wells and double wells, have been investigated from a kinetic point of view. Derivations and applications have been in connection to along-B wells and double wells that may exist around Earth, mainly in equatorial regions. These wells are of electric (ambipolar)-gravity and magnetic origin, and they were studied alone and in combination. Collisions between the ion populations and the background plasma have been taken account of using a simplified collision term that to some extent made it possible to derive analytic solutions of the ion kinetic equation, even when time dependencies were included in the collision parameters. The kinetic equations solved were one-dimensional (along-B), but time-dependencies included in collision parameters may mimic effects of a changing background due to say equatorial motion. Some examples of evolutions have been given graphically and shows that peculiar behaviours may arise when proper conditions are met, as "breathing" of the distribution function as time goes on, and, when an additional oscillating force field is included, steps towards development of strange attractor support of distribution functions in a rather short time. The results obtained may have relevance to other plasmas where similar or analogous wells and double wells may exist.

References

[1] Kelly,M.C., 1989, *The Earth's Ionosphere*, Academic Press.

[2] Leer,E., Lie-Svendsen,Ø., Olsen,E.L. and Hansteen,V.H., 1996, J.Geophys.Res. **101**,17207.

[3] Lie-Svendsen,Ø. and Rees,M.H., 1996, J.Geophys.Res. **101**, 2415.

[4] Øien.A.H.,1999, J.Plasma Physics, **61**,part 5, 735.

[5] Baumjohann,W. and Treumann,R.H., 1996, *Basic Space Plasma Physics*, Imperial College Press.

[6] Fälthammar, C.-G., 1973, *Motion of Charged Particles in the Magnetosphere*, in, *Cosmical Geophysics* (ed. A.Egeland, Ø.Holter and A. Omholt), Universitetsforlaget, Oslo.

[7] Chandrasekhar,S., 1943, Rev.Mod.Phys., **15**, 1.

[8] Landau,L.D., 1936, Physik.Z.Sowjetunion, **10**, 154.

[9] Bogolioubov,N.N., 1946, *Problems of a Dynamical Theory in Statistical Physics*, State Technical Press, Moscow. English translation in *Studies in Statistical Mechanics*, vol.1(ed. J.de Boer and G.E.Uhlenbeck). North Holland Publishing Company, Amsterdam,1962.

[10] Nayfeh,A.H., 1973, *Perturbation Methods*. John Wiley & Sons.

[11] Guckenheimer,J. and Holmes,P.,1983, *Nonlinear Oscillations, Dynamical Systems, and Bifurcation of Vector Fields*. Springer New York.

[12] Strogatz,S.H., 1994, *Nonlinear Dynamics and Chaos*. Addison-Wesley.

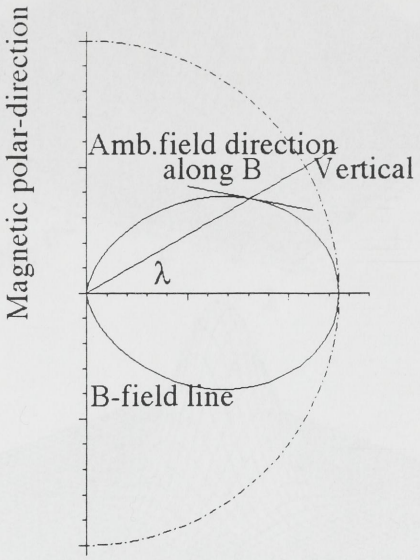

Fig.1: Ambipolar field direction along dipole magnetic field. Cross section of magnetic equator plane showing magnetic field line, vertical at λ-magnetic latitude and line along magnetic field.

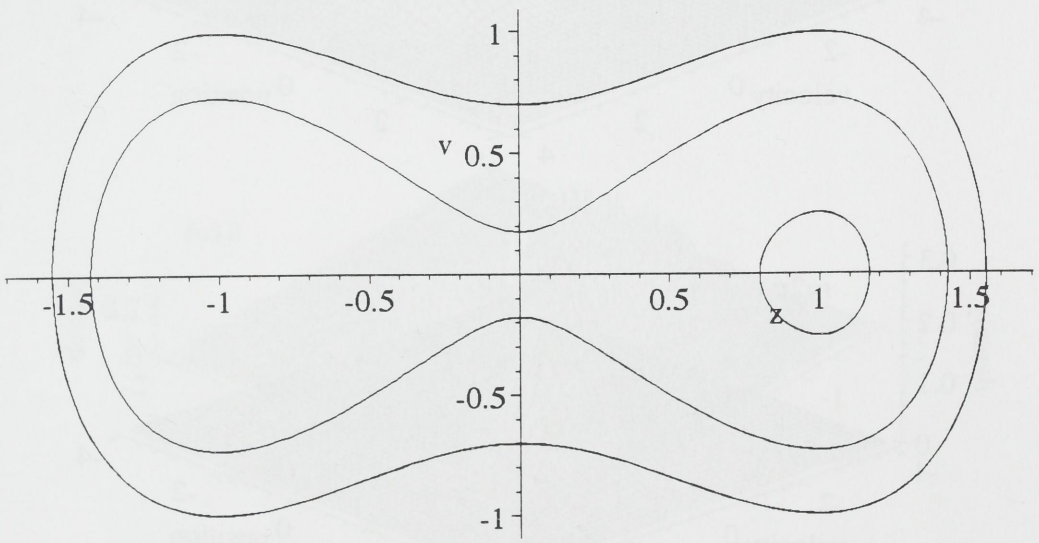

Fig.2: Phase plane curves of double well, wells at $z=\pm 1$, $\alpha_1 = 19/13$, $\alpha_2 = 2/13$, cf. Eqs.(29) and (56) and text.

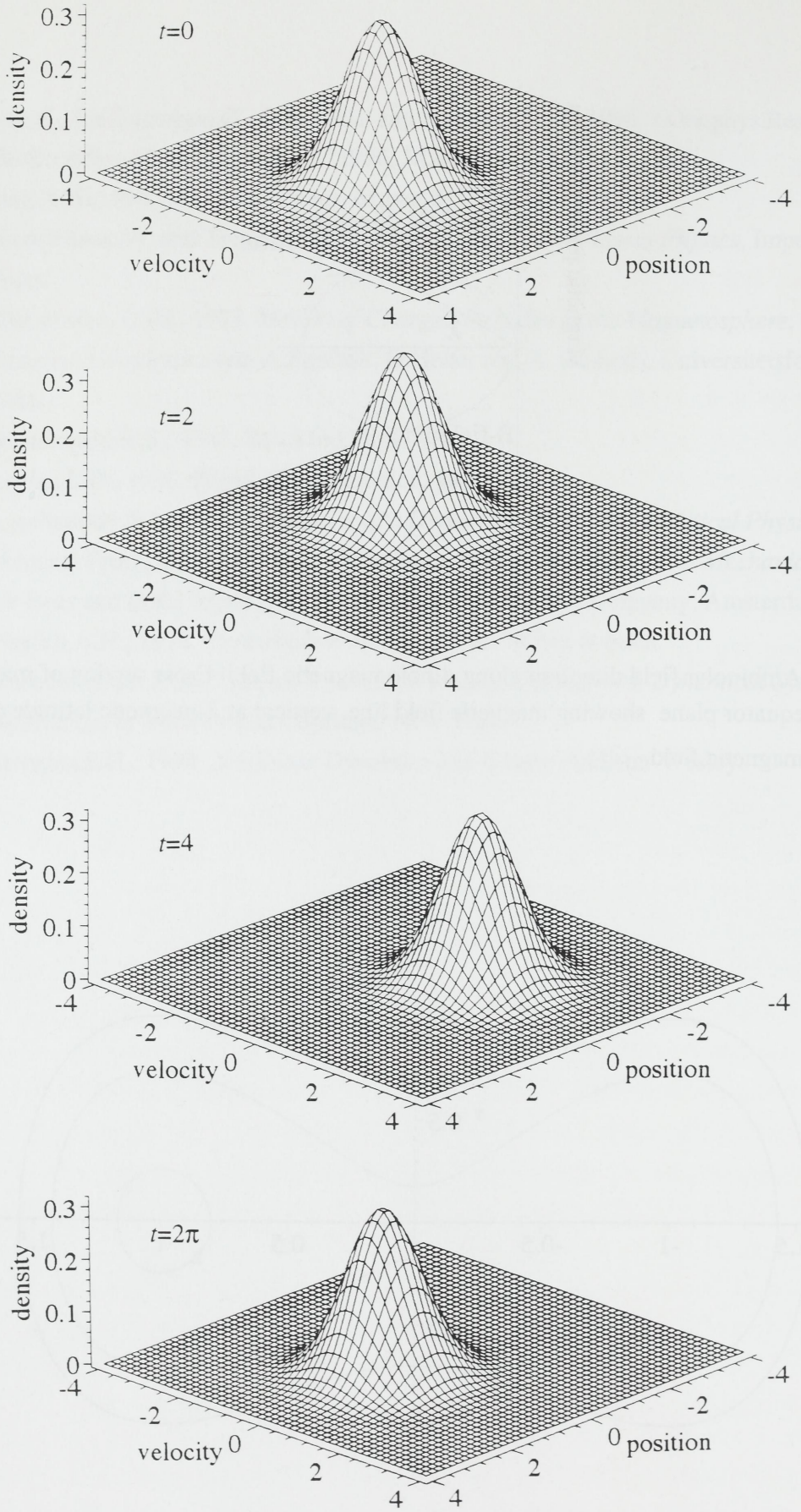

Fig.3: Distribution function of light ions at t=0, 2,4 and 2π for harmonic well (ω=1) in collisionless case. Initial ($t = 0^+$) bell shaped distribution around (z, v_z)=(1,0), M=1, cf. Eq.(52) and text.

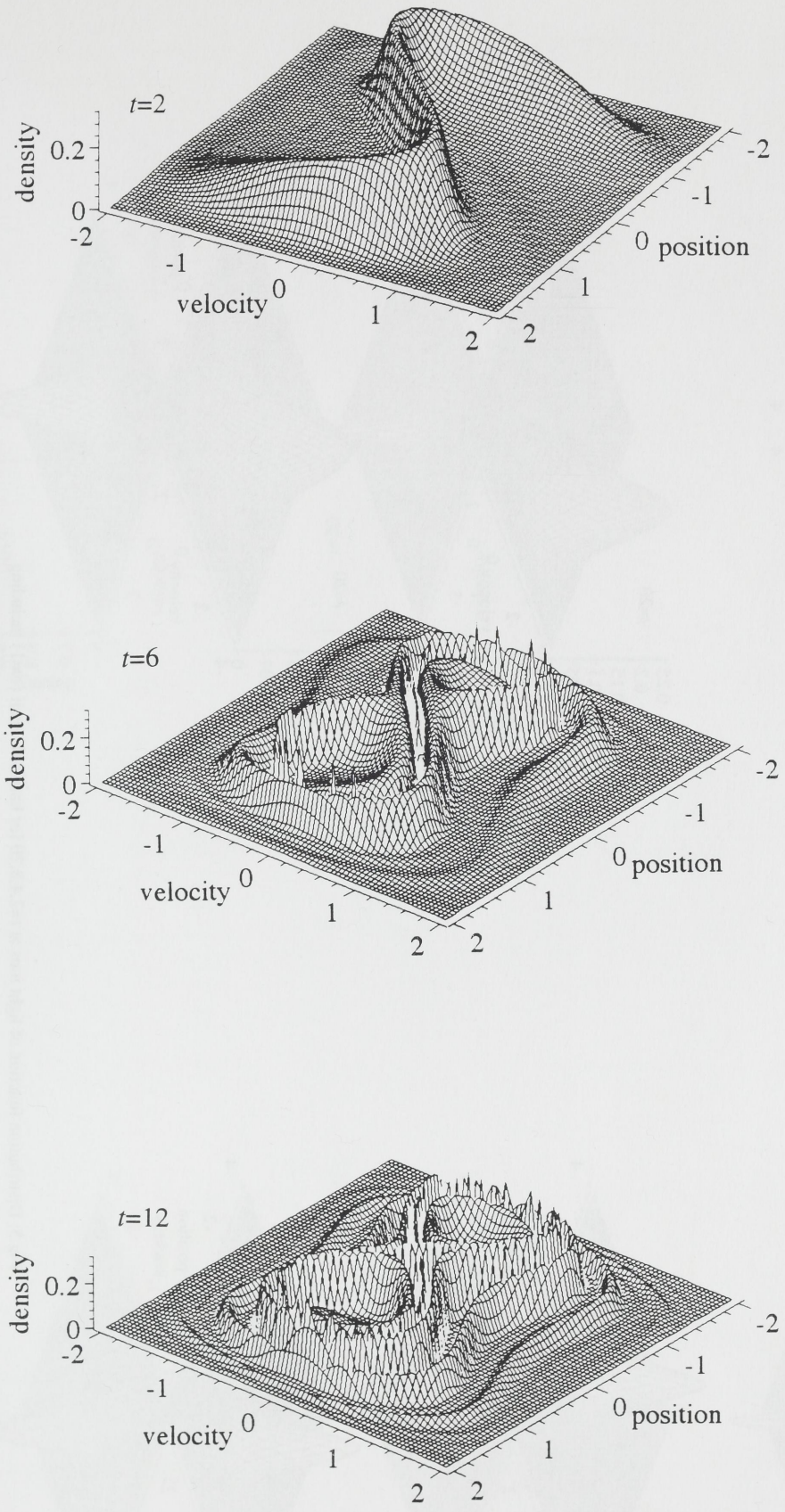

Fig.4: Distribution function of light ions at t=2,6,12, for double well in collisionless case. Wells at z=±1. Initial ($t = 0^+$) bell shaped distribution around (z, v_z)=(0,0), M=1, $\alpha_1 = 19/13, \alpha_2 = 2/13$, cf. Eq.(58) and text.

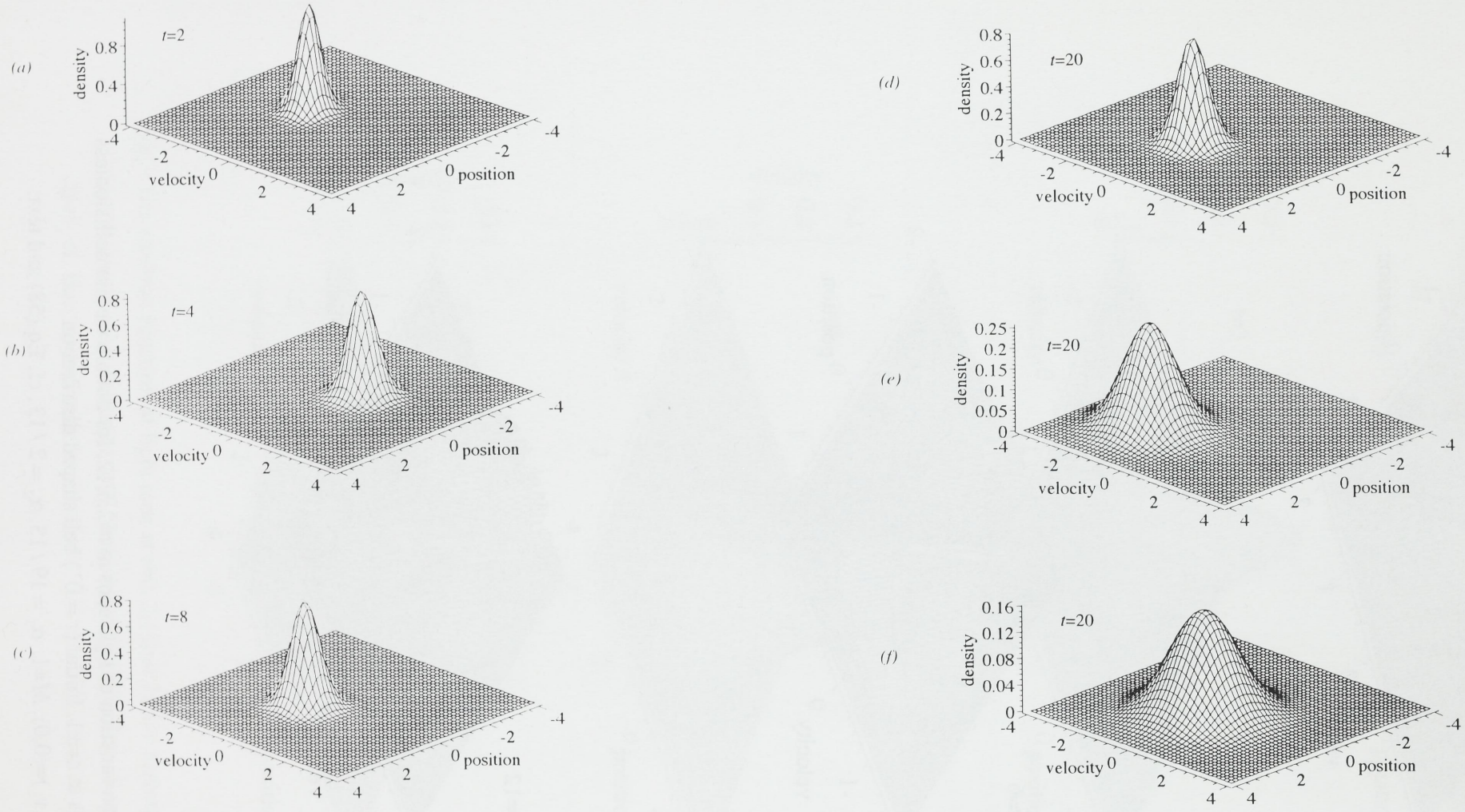

Fig.5: Distribution function of light ions at t=2,4,8,20 for harmonic well (ω=1) including effects of collisions, which slowly die away for increasing time ($\beta = e^{-0.2t}$, $q = 0.2e^{-0.2t}$) and an oscillating field, ($0.5\cos(0.5t)$), (a)-(d). Initial ($t = 0^{+}$) delta function distribution at (z, v_z)=(2,0), M=1, cf. Eqs.(95) and (101). (e): Distribution at t=20 if collisional friction instead $\beta = 0.2e^{-0.2t}$ from start as compared to (a)-(d). (f): Distribution at t=20 if instead $q = e^{-0.2t}$ from start as compared to (a)-(d).

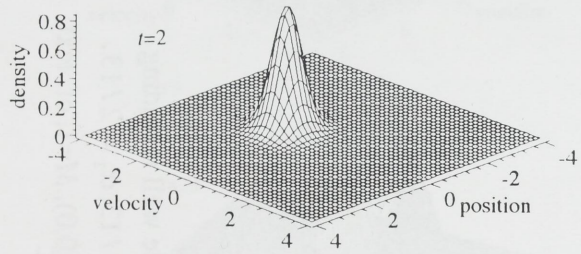

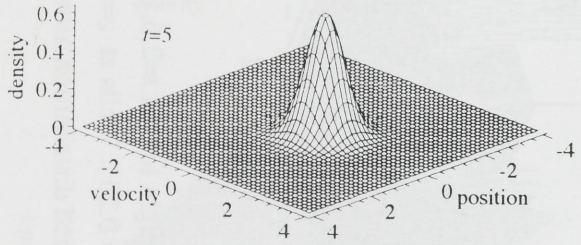

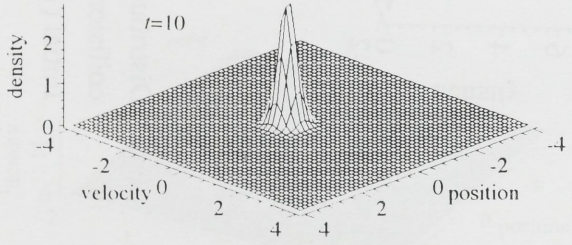

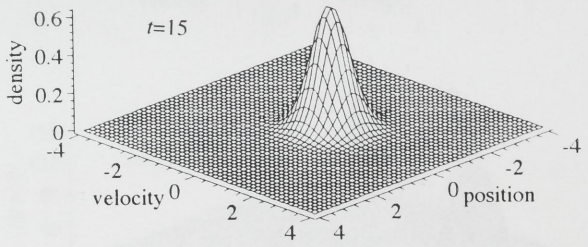

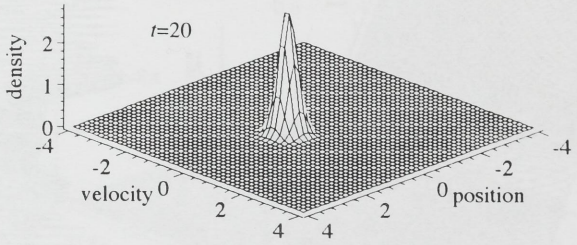

Fig.6: Distribution function of light ions at t=2,5,10,15,20 for harmonic well (ω=1) including effects of collisions and an oscillating field, ($0.5\cos(0.5t)$). Collisional friction held constant (β=1) while $q(t)$ is turned periodically on and off (nearly), q=0.25, q=0.05, at a period equal to 10. Initial ($t = 0^+$) delta function distribution at (z, v_z)=(2,0), M=1, cf. Eqs.(95) and (101).

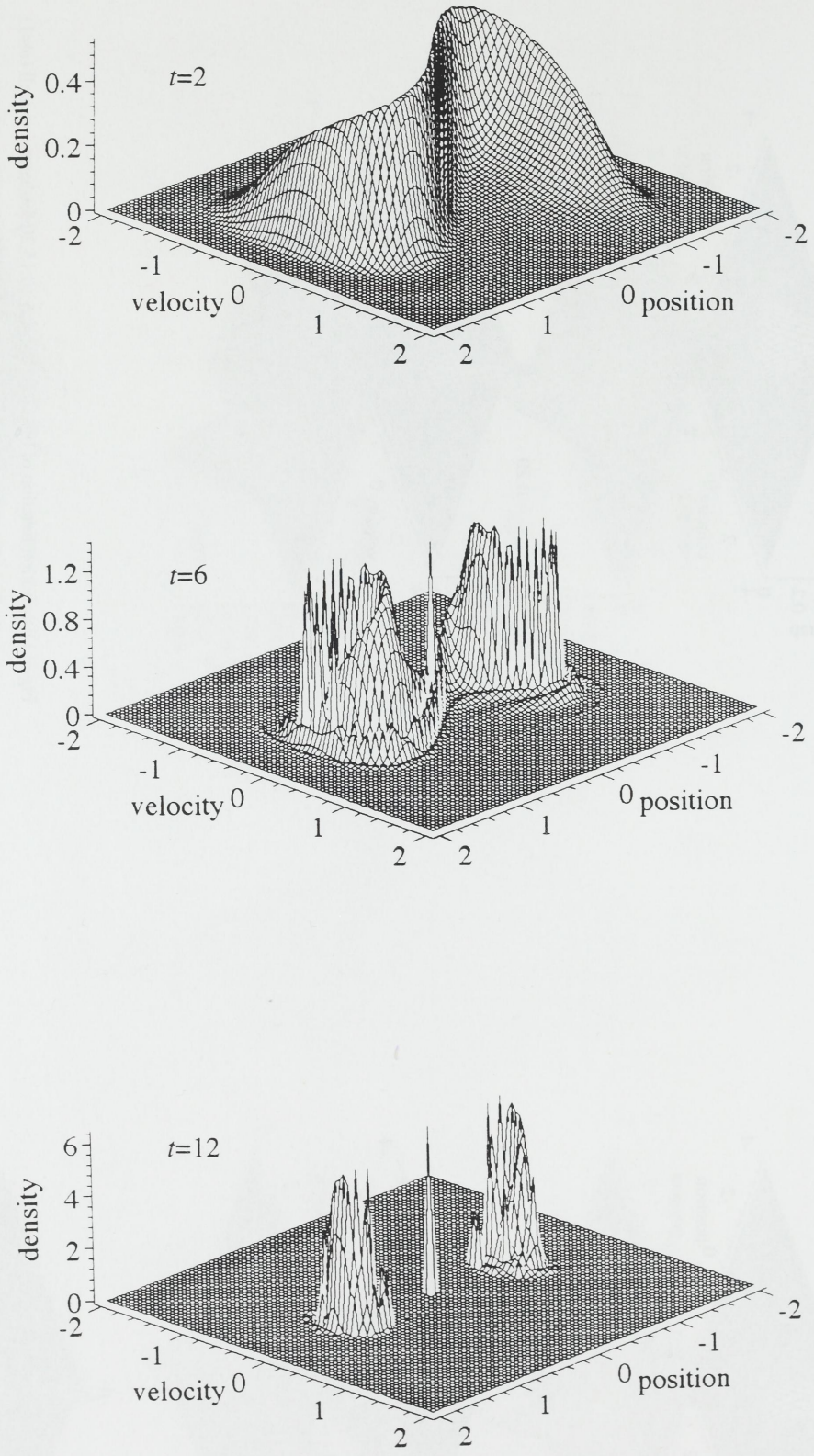

Fig.7: Distribution function of light ions at t=2,6,12, for double well including collisional friction ($\beta = 0.25$). Wells at z=±1, $\alpha_1 = 19/13, \alpha_2 = 2/13$. Initial ($t = 0^+$) bell shaped distribution around (z, v_z)=(0,0), M=1, cf. text.

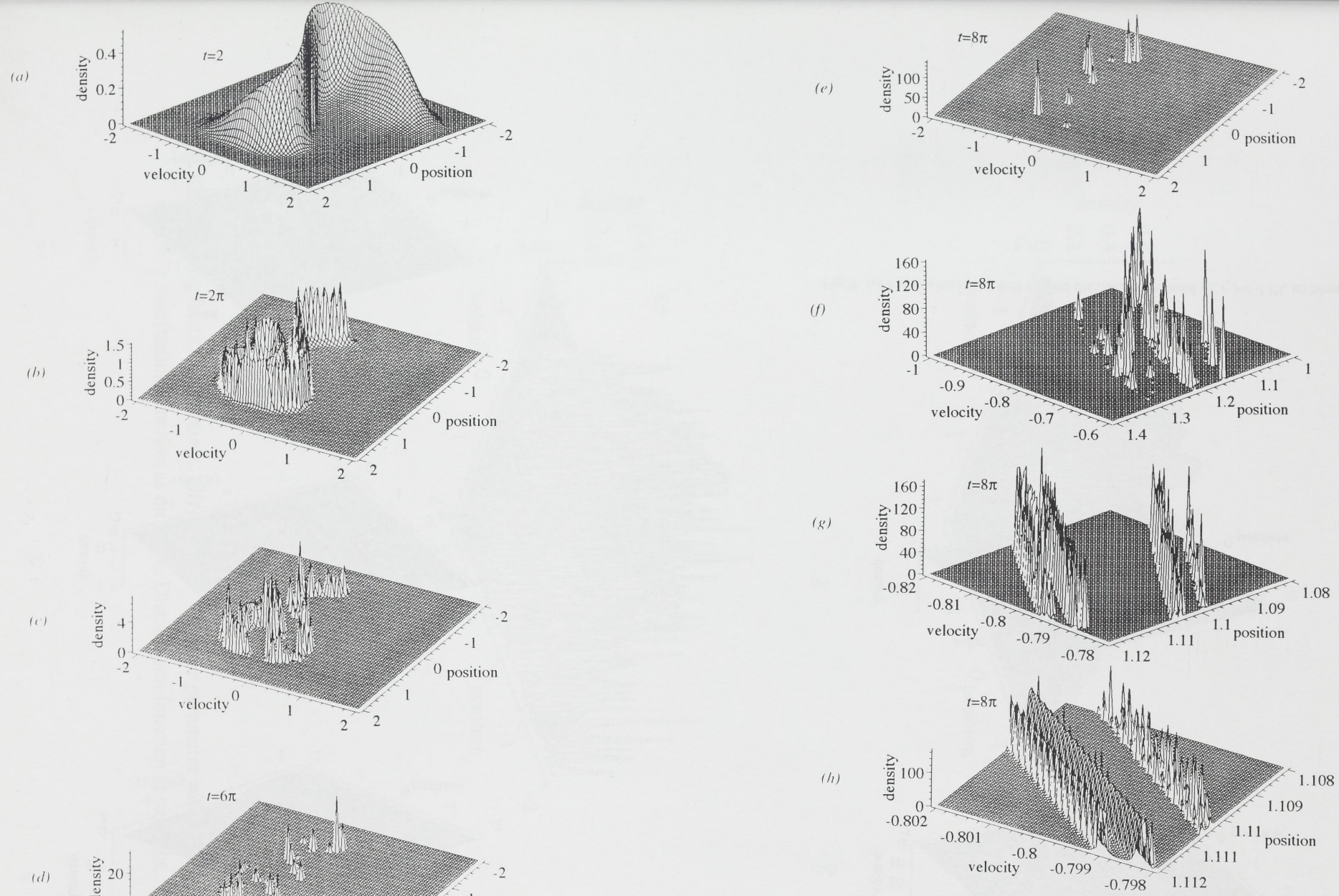

Fig.8: Distribution function of light ions at t=2,2π,4π,6π,8π for double well including collisional friction ($\beta = 0.25$) and oscillating field ($0.4\cos(t)$). Wells at z=±1, $\alpha_1 = 19/13, \alpha_2 = 2/13$. Initial ($t = 0^+$) bell-shaped distribution around (z, v_z)=(0,0), M=1. (f), (g) and (h): Successive blow-ups of distribution function.

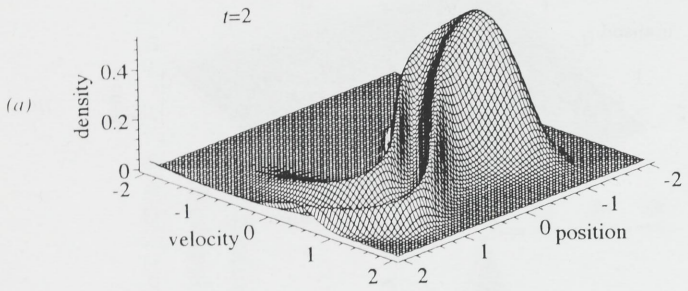

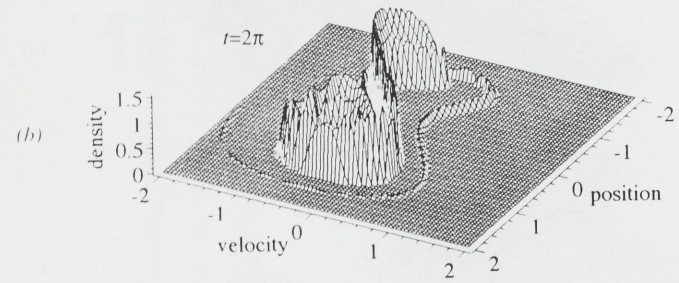

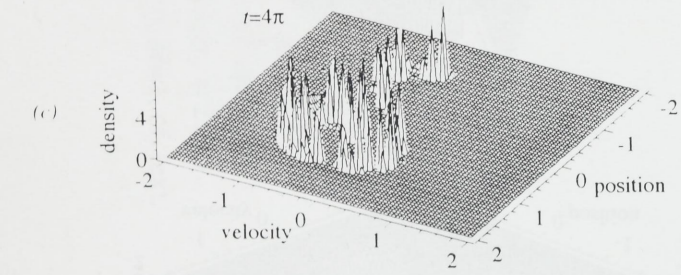

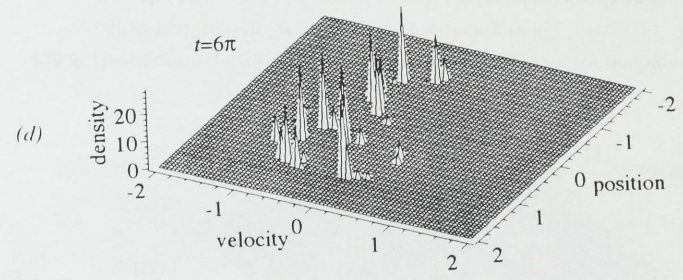

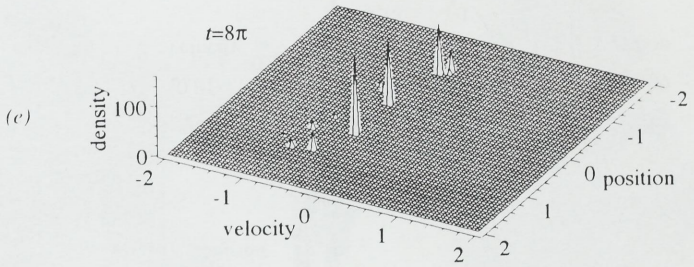

Fig.9: As Fig.8 with initial bell shaped distribution around (z, v_z)=(-1,0), no blow-ups.

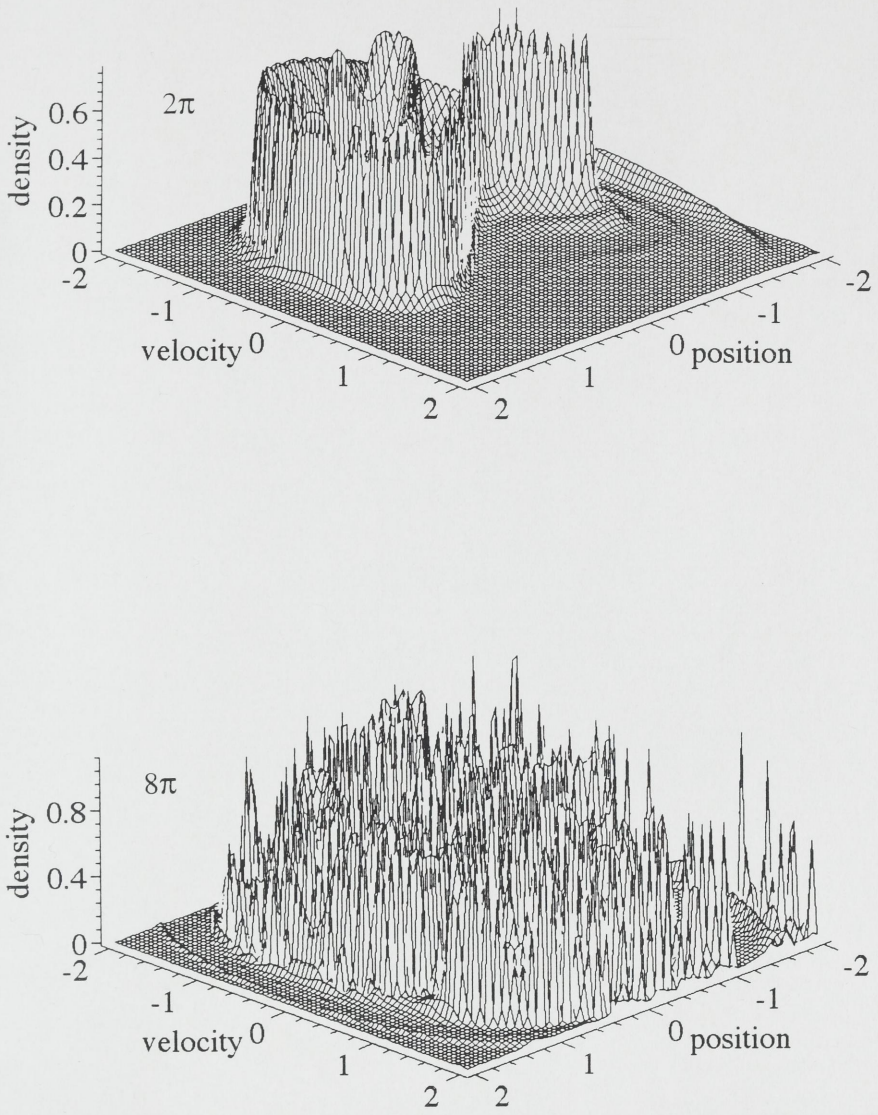

Fig.10: Decaying friction coefficient, $\beta(t) = 0.25e^{-0.2t}$, other parameter values, and initial ($t = 0^+$) distribution function as on Fig.8. Distribution function at t=2π,8π.